Research Article – Vol. 02, Issue 01, No. 03

Advanced in Engineering and Intelligence Systems

Journal Web Page: https://aeis.bilijipub.com

Investigating the Two Optimization Algorithms (GWO and ACO) Coupling with Radial Basis Neural Network to Estimate the Pile Settlement

Ehsanolah Assareh[1,*] , Reza poultangari[2]

[1] *School of Chemical Engineering, Yeungnam University, Gyeongsan 38541, South Korea*
[2] *Department of Mechanical Engineering, Dezful Branch, Islamic Azad University, Dezful, Iran*

Highlights

- A rich dataset of pile settlements is gathered from various kinds of literature.
- A pre-process was implemented to prepare the dataset.
- A robust model is developed based on radial based neural network.
- The robustness of the model improved by coupling the network with the grey wolf and ant colony optimization algorithm.

Article Info

Received: 12 December 2022
Received in revised: 27 March 2023
Accepted: 19 March 2023
Available online: 28 March 2023

Keywords

Pile Settlement;
Radial basis function;
Grey wolf optimization;
Ant colony optimization;
RMSE.

Abstract

Immunizing projects such as piled bridges entail considerations that ensure safety over the operation period. Pile Settlement (PS) which seems one of the most critical matters in constructional project failure, has attracted experts' attention to be predicted before starting projects with piles. The variables to appraise the pile movement would help us determine the perspectives after and during loading. Theoretical ways to calculate the pile movement mathematically have been adopted to model the PS, mostly by using artificial intelligence (AI). This paper has aimed to estimate the pile settlement rates based on pile samples. For this reason, a new hybrid model containing a Radial Basis Function Neural Network (RBFNN) joining with Grey Wolf Optimization (GWO) and Ant Colony Optimization (ACO) were used in a framework. In fact, optimizers utilized for calculating the neuron number of hidden layer in RBFNN at optimal level. In Malaysia, the Kuala Lumpur transportation network was investigated to examine the pile movement based on ground conditions and properties through the developed hybrid RBF-GWO and RBF-ACO algorithm. Evaluating each framework's performance was done via the indices. So, the RMSEs of RBF-GWO and RBF-ACO reached values 0.5176 and 0.6562, respectively, and the MAE showed the rates 0.2583 and 0.3386, respectively. The correlation R-value also showed the RBF-GWO suitable accuracy with 1.23 percent higher than another model. Therefore, results have implied the RBF-GWO desirable performance to estimate PS.

1. Introduction

Engineers must consider the ground condition resulting from erosion, tectonic activities, or nature manipulation by mankind as deep-excavations and tunneling on settlement of pile and its foundations. Many types of research have extensively examined the reflection of piles to changing ground status that has led to pile movements [1]– [4]. Whereas the response of pile for issues dominated by ground settlements has not yet been completely characterized [5], [6]. The investigation of soil-pile interaction was done based on both pile settlements related to distortions and damage and pile axial forces corresponding to the potential for pile cracking [7]– [9]. The subsidence of pile seems to relate to factors of loads on the pile, the length ratio of the pillar to the diameter of it, the UCS parameter in rock, the ratio of the length of the pillar in the soil to rock, and the N_{SPT}, as the variable for the soil penetration [10], [11]. Research classified pile foundations into two types: (1) small piled rafts and (2) large piled rafts [12]. The first ones are those in which the capacity of

* Corresponding Author: Ehsanolah Assareh
Email: Ehsanolah.assareh@gmail.com

bearing the unpiled raft is insufficient in order to add piles to achieve a suitable factor of safety against bearing capacity. The Br parameter as the width of a small piled raft is generally narrow compared to the length Lp of the piles (Br=Lp<1), and these foundations have rigidity high with any issues related to differential settlement. Large piled rafts (Br=Lp > 1) are those in which the raft bearing capacity is generally sufficient, but subsidence of raft often is more than the acceptable magnitude. The analysis and design of piles are complex because of their sophisticated (raft-pile-soil) interaction and their foundation in response to the discrepancy of load, structural configuration, and soil properties. Micro-scale studies of experimental types including discriminating experiments have examined the treatment of pile foundation designs [13]– [15]. Large model tests or macro-scale experiments are essential to fully get all sides of pile behavior. Such experimental macro-scale researches are costly and hard to enact. Therefore, the literature contains various simplified and numerical methods for predicting pile behavior over movement.

A great number of researchers have proposed simplified methods to foresee the early load-settlement response of pile motion considering the elastic behavior of soil. Some simple procedures study the movements of piles, where the capacity of the bearing of the pile foundation system is added to control excessive settlement [16]. By other simplified solutions, load transferring between the piles and foundation and soil beneath is considered the interaction between piles and ground below [17], [18].

Many studies have examined the discontinuous resistance at the base of the pile and presented the radial force at the circumference of the pile. It is determined through a function of fictional stress [19]. As reflected by some researchers [17], the studied piles propose a semi-analytical solution to simultaneously check the heterogeneity and non-linearity of the soil. In addition, another paper proposes a method to analyze the lifting capacity in the pillar and build a theoretical function to study the coefficient of lateral earth pressure [20], [21]. All of the referred papers chiefly evaluated the motion of the pillars, but none were used straightly without a ground response model.

The solution so-called Artificial neural networks (ANN) with practical ramifications via a great deal of studies such as Che et al. [22], Liu et al. [23], Shanbeh et al. [24], Lee and Lee [25], and Hanna et al. [26], have been chosen in forecasting some parts of the complicated matters of the pile in the capacity of bearing [27]. The settlement parameters of the pile and the friction and bearing capacity of the pile are being examined by modern solutions. Many studies have deployed training data collection to produce predictive models for testing pile load capacity and settlement of pile amount. The collection of data for training was chosen for the neural network from a wide range of surveys in the dynamic field [11], [28]. One study[29] using the neural network has strived to formulate the outputs of load-settlement behavior of piles installed into rock. The data set associated with training phase was collected from the actual pile reports. ANN suggested computed the outcomes more precise and reliable than formulas of traditional one. Another paper [30] used ANN frameworks to appraise capacity of pile-bearing.

The present paper has strived to develop practical frameworks estimating the pile settlement rates. To this end, new hybrid models containing a Radial Basis Function Neural Network (RBFNN) joining with Grey Wolf Optimization (GWO) and Ant Colony Optimization (ACO) were used in two frameworks. In fact, optimizers utilized for calculating the neuron number of hidden layer in RBFNN at optimal level and evaluate an integrated framework as a radial basis function (RBF) neural network accompanied by two capable optimization algorithms. The mentioned two algorithms were considered as there are not any researches using RBFNN coupling with the algorithms. Also, the capabilities of them can be found in many researches [31]– [34]. The novelty of the present study can be defined as using algorithms to estimate the pillar settlement installed in rock. The testing data collection for pile movement analysis and the ground properties had been gathered from the Malaysia transport project in Klang Valley Mass Rapid (KVMRT) network in Kuala Lumpur. The optimizers coupled with the neural network of radial basis function (RBF) have been prospectively surveyed for many complicated issues because of the simple, smart, and appropriate capabilities. Both techniques are well-known in the academic world as a way of machine learning, such as the specialization fields on energy transformation, biology, image analyzing [35]– [38]. Generally, developing boosted models such as hybrid and ensemble ones can lift the capabilities of them in tunning the main predicting models while some experts have great tendency for hybrid than ensemble. The proposed framework is meant to collect data by testing penetrating and loading static by real ground measurements. With this regard, the load on the column, the ratio of the column length to the diameter of the column, the UCS used in the rock, the ratio between the length of the column in the soil and the rock, and finally, the N_{SPT} synthesizing input data to check settlement. Column sunk into the ground [39].

A series of researches have reported the prospective use of RBF in engineering fields, such as prediction in precipitation rate by compounding the neural network of

RBF and optimization algorithms [40], [41]. This study also strives to calculate the number of neurons at the optimal rate in the middle layer called hidden as well as the propagation speed. In fact, using artificial intelligent-based techniques are getting common in civil engineering fields to save invests, energy, at the same time, increasing the accuracy of predictions.

The parameters are defined as the final capacity bearing, the ratio of the column length in the soil to length under rock subsurface, plus pile settlement (PS) as the target value, the strength of uniaxial compressive, total length to cross-section diameter, testing penetration in standard status. To investigate and evaluate the fitness of the models' predicted values as pile settlement rates, the R2, RMSE, OBJ, and MAE indices were considered for the modeling process.

2. Methodology

2.1. Preparing primitive dataset

The Klang Valley Mass Rapid Transit (KVMRT) project in the city of Kuala Lumpur, the country of Malaysia, got planned to control the city transportation management and got opted as a study case for this research. The referred project has many installed piles supporting carrying the load masses through pile structures to prevent the project from collapsing. The location of the KVMRT as a study area is exhibited in Figure 1. Lots of piles on various rocks such as granite, limestone, and phyllite can be found. In the research, 96 piles were recorded from the granite of Santorias class predominates. Data on pile location and material existing underground have been vitally discovered as geologic characteristics. The underneath the soil layer, as found, is made up of leftover rock fragments. Thus, the rock in deep underground within the data collected is forecasted between 70 centimeters and a depth rate greater than 1400 m. Moreover, the compilation of sample data has introduced as follows:

a) Lower and higher UCS magnitudes according to ISRM, in the range 25 and 68 Mega Paskal (MPa) respectively, [42].
b) The dominant soil is composed of hard sandy mud plus a minimum and maximum rate of N_{SPT} of 4 and 167 blows per 300 mm, respectively.
c) The observed masses of rocks are moderate to extremely variable
d) Bore gathered information of piles in 16.5 meters, soils highly weathered and common soils commonly with silt.

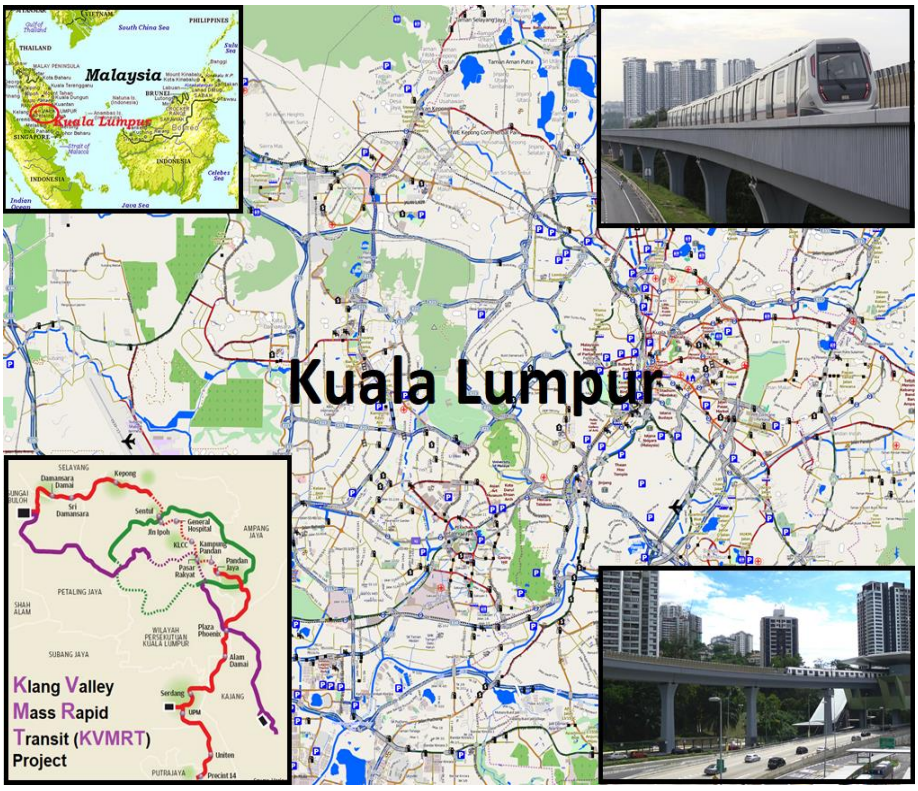

Fig. 1. The study area of KVMRT, Malaysia

Arranging the principal data based on the entering ones must appear as the primary stage to estimate the model's outputs. Considering parameters affecting outputs of the model seems necessary for the proposed framework. Pillar Dynamic Inc. carried out the above ground analyses, which performed the pile analysis. Nonetheless, the pile length and the cross-sectional diameter of the pile, as previously stated, are involved as parameters to predict the pile settlement during the pile loading period. In this regard, two options to consider the ratio of pile length in sheets of soil to pile length in rock level (L_s/L_r), and the ratio of all lengths of a pillar to its diameter (L_p/D) are opted to analyze the current state of pile geometry. Regarding the solving process, the rate of the N_{SPT} is also used as input data to use the ground situation. Additionally, the UCS of soil is entered as primary data to the model to estimate the pile motion. Moreover, piles would have a straight consequence on the pile displacement over the loading stage. The input data assign the ultimate bearing capacity of the pile called Qu.

Nevertheless, some information is supposed to be used to estimate and survey the settlement of piles. The entering data results of the present research, plus the target values of pile settlements to reveal ranges, are shown in Table 1. The histograms of the input and target values of pile settlements are also brought in through Figure 2.

Table 1. Specification of studied DGs.

Variable	L_p/D	L_s/L_r	N_{SPT}	UCS (MPa)	Q_u (KN)	PS (mm)
Max.	32	32	166	68	42701	20.1
Min.	4	0.3	3	25	12409	4.5
St. Dev	7	7	59	12	8030	3.7
Median	14	4	104	43	21898	11
Avg.	15	7	80	43	24540	11

As shown via Fig. 2, the histogram plots attempt to indicate the frequency of each variable as Lp/D, Ls/Lr, Q_u, N_{SPT}, UCS are diagnosed to impact the settlement of pile.

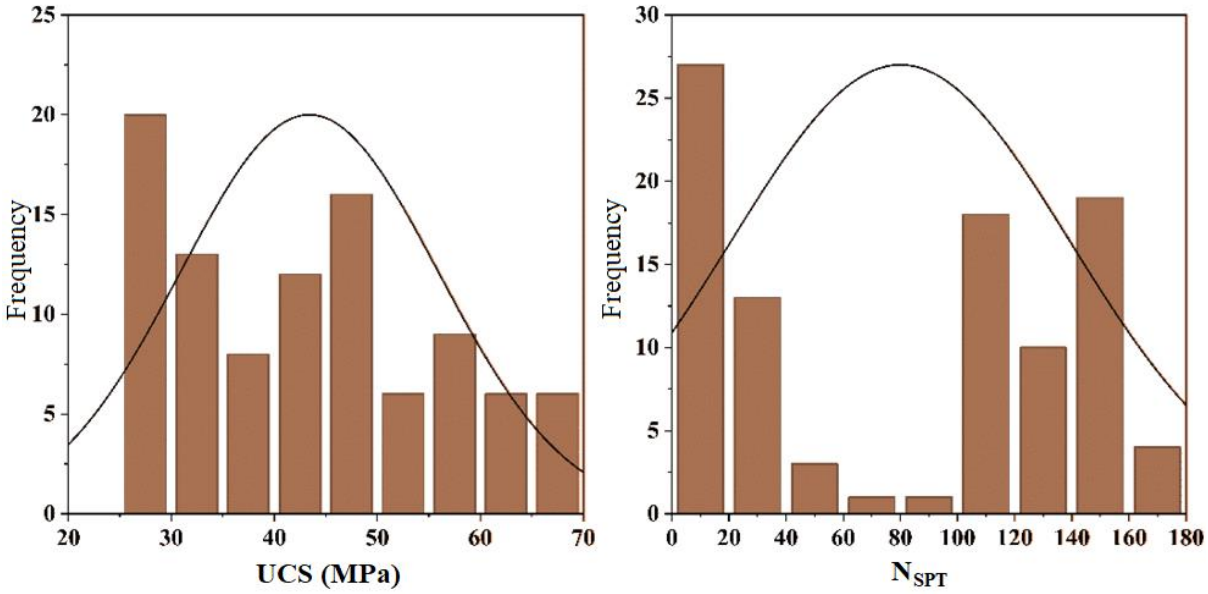

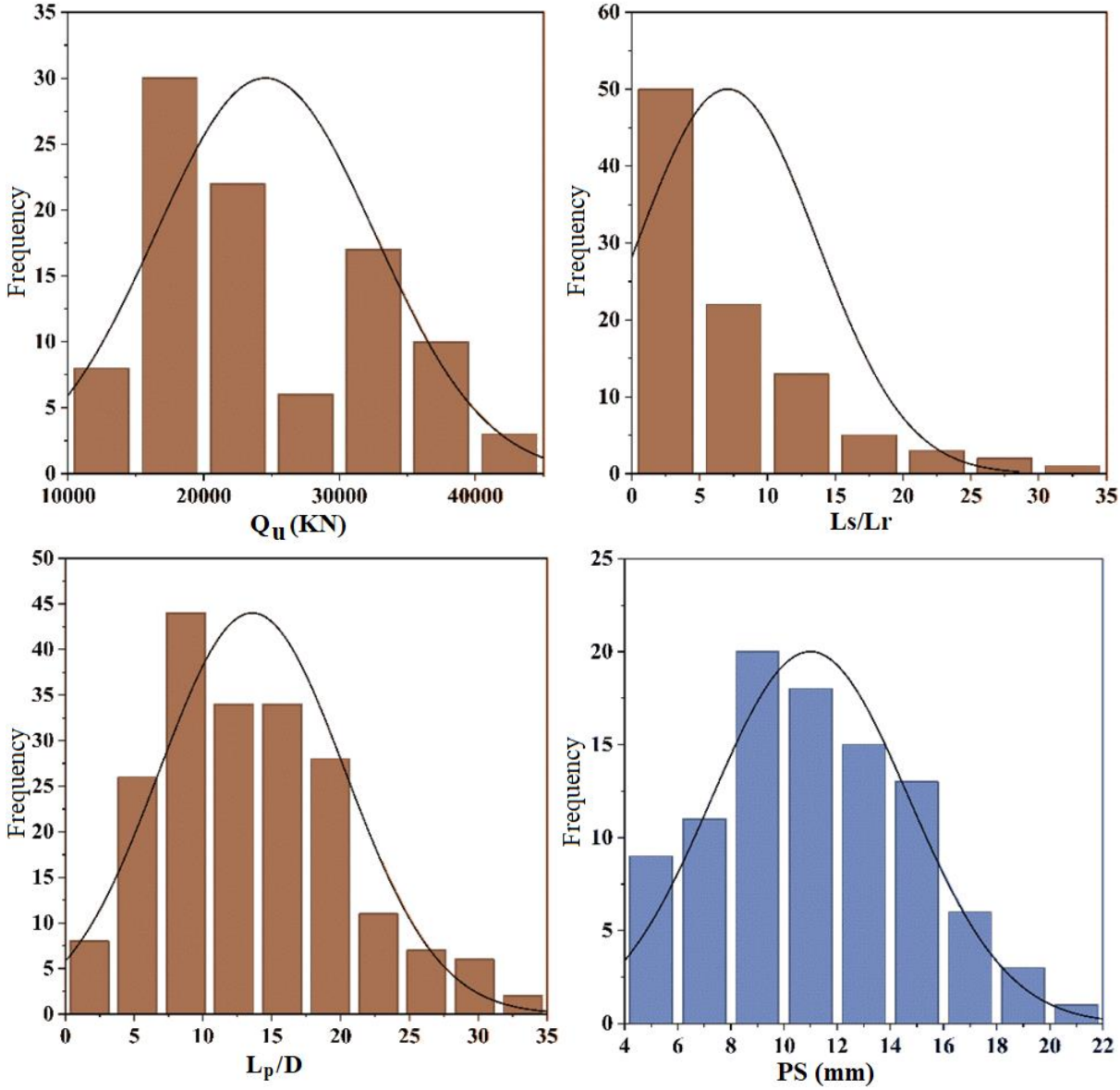

Fig. 2. The histograms of the primitive dataset to model the pile settlement

2.2. RBF; neural network of Radial basis Function

This neural network, owning a simple structure and great capabilities, is a suitable and quick estimator [43]. The proposed neural network of RBF consists of the following layers: I) input layer, II) hidden layer, and III) output layer. The number of neurons inside the hidden layer is the main aim of this research to compute at an optimal rate with low cost and complexity of the network to improve the accuracy. The proposed RBF amplitude is simply separated from the CenterPoint. This is usually based on using the Euclidean rule. A complement of principal functions was operated to guide the vector between input and output. The formula of Gaussian is used as the math operator mainly by several methods of infinity and understandability. The lattice result for the Gaussian formula, which acts as an essential function, is brought up as following equations:

$$\Phi (X, X_j) = \Phi (|| X-X_j||), X= [x_1, x_2, x_{3...}, x_n] \quad (1)$$

$$\Phi (r)= e^{-\frac{r^2}{\sigma^2}} \quad (2)$$

$$y_k = \sum_1^m \omega_{ik} \Phi(X, X_i) \quad (3)$$

For the abovementioned relations, y_k represents the layer of output, the variable of X_i denotes the X center, σ shows the smoothness, X shows the i th layer of the input

vector, || f || represents the norm of Euclidean, Φ represents the basic function.

2.3. GWO; Grey Wolf Optimization

Grey Wolf Optimization is known as the algorithm of meta-heuristic [44]. Grey wolves pass their life with intensive social treatments. Leader wolves are named alpha, beta superior, and omega ones as a scape GWO. Over the rank belonged to wolves, they have tracked encircling, invading, then hunting. This characteristic is formulated mathematically as following equations [44].

$$\vec{D} = \left|\vec{C}.\overrightarrow{X_P}(t) - \vec{X}(t)\right| \quad (4)$$

$$\vec{X}(t+1) = \overrightarrow{X_P}(t) - \vec{A}.\vec{D} \quad (5)$$

$$\vec{A} = 2\vec{a}.\overrightarrow{r_1} - \overrightarrow{a} \quad (6)$$

$$\vec{C} = 2.\overrightarrow{r_2} \quad (7)$$

Wherein, $\vec{X}$ represents the position of grey wolf location; $\overrightarrow{X_P}(t)$ the vector of prey position; t shows the time, a represents reduction from 2 to 0 linearly; $\overrightarrow{r_1}$ and $\overrightarrow{r_2}$ shows the random vectors monotonously distributed between 0 and 1.

Generally, the hunting way of wolves is modeled through those close to the prey at enough distance. Then, the remaining ones based on alpha, beta, and omega positions would find food positions. Locations of preys are estimated via the average wolves' situations via the following equations:

$$\begin{Bmatrix} \overrightarrow{D_\alpha} = \left|\overrightarrow{C_1}.\overrightarrow{X_\alpha} - \vec{X}\right| \\ \overrightarrow{D_\beta} = \left|\overrightarrow{C_2}.\overrightarrow{X_\beta} - \vec{X}\right| \\ \overrightarrow{D_\delta} = \left|\overrightarrow{C_3}.\overrightarrow{X_\delta} - \vec{X}\right| \end{Bmatrix}, \quad \begin{Bmatrix} \overrightarrow{X_1} = \overrightarrow{X_\alpha} - \overrightarrow{A_1}.\overrightarrow{D_\alpha} \\ \overrightarrow{X_2} = \overrightarrow{X_\beta} - \overrightarrow{A_2}.\overrightarrow{D_\beta} \\ \overrightarrow{X_3} = \overrightarrow{X_\delta} - \overrightarrow{A_3}.\overrightarrow{D_\delta} \end{Bmatrix}, \quad (8)$$

$$\vec{X}(t+1) = \frac{\overrightarrow{X_1} + \overrightarrow{X_2} + \overrightarrow{X_3}}{3}$$

Next to the prey position, later stage would be the exploitation, which is calculated from the $\vec{A}$ vector. If the magnitude of parameter a changes from 2 to 0, the situations of these animals displace to the prey position. Further, the value of C could change the situation of prey and the strictness of the hunting procedure. The value of A as being more than 1 convinces the grey wolf to get a part of the prey and find an appropriate one. Moreover, this procedure cycles for the whole of wolves, in which the optimum location can finally be found.

2.4. ACO; Ant Colony Optimization

Ant Colony Optimization (ACO) uses the treatments of blind ants that developed a basis of population heuristic technique, as ACO [45], [46]. Materials such as pheromones have been known substances that deposit on the earth that ants carry food from their source to their nests. They exploit the mentioned way to non-straightly convey data about the closest path among the nest and food source and operate a chemical substance's strength (pheromone) to assess its capability for the path registered.

The ant number as m (colony size) got opted. Then, the initial severity of the right substances (pheromone) that is called τ_o determined for the whole of e_{ij}. The Pheromone primitive severity is usually calculated with Eq. (9) [47]:

$$\tau_0 = \frac{1}{nL_{nn}} \quad (9)$$

That L_{nn} denotes the variable of tour length among n number colonies (cities) developed through adjacent heuristic vicinage [48]. Satisfying these tasks' restrictions is not important by task [33], [49]. Ant colonies move between the vertices to build a solution to the problem. Given any preselected design variables as i, a probabilistic local decision policy is applied via ant k to opt for an accessible choice to variables. The Transition Rule of Random Proportional was defined [50], [51], that this policy of decision is determined by two parameters: visibility (attractiveness of movement) and level of the trail (pheromone severity). Visibility preliminarily shows the desire for movement, presents an artificial spectacle for choosing the closest path from options without experience or observation of movement, and indicates the experience has gained at that stage. The transition rules that k (ant) uses for opting a choice is:

$$p_{ij}\ (k,t) = \frac{[\tau_{ij}(t)]^\alpha [\eta_{ij}]^\beta}{\sum_{j=1}^{J_i} [\tau_{ij}(t)]^\alpha [\eta_{ij}]^\beta} \quad (10)$$

Wherein p_{ij} denotes the expectancy which the i^{th} point of decision of choice j is chosen by ant k in the t number of iterations; τ_{ij} indicates a rate of trail in choice e_{ij} at the t iteration, η_{ij} is the ant scope of the showing the selecting choice j cost locally over the point of decision of i^{th} (η_{ij} =1 divide to c_{ij}); α as well as β denotes two variables modifying proportional level importance of trail versus scope.

The ACO method employs several concepts from theory of graph. Objective function that violates the induced restrictions are penalized via a static way:

$$f_p(\psi^k) = f_(\psi^k)[1+\Phi]^{\varepsilon} \quad (11)$$

In Eq. (9) $f_p(\psi^k)$ denotes the function of goal penalized by k^{th} ant; the variable of Φ shows penalty totally and the penalties sum of deflection plus force; ε represents an exponent of positive penalty, which is fixed in the static penalty way modified relatively to the violation extent in the restrictions in adaptive penalties [48]. Ants build m ways incrementally to issue via selecting solutions to move among nodes of decision, to observe every node, when the whole of nodes is observed and returned to their original state. Until they get back to starting position, ants finish a course that everyone creates its trial way, ψ^k. The concept of one *cycle* seems finished if ants with the number of m accomplish courses and build the practical way of m.

An iteration reaches an end if m ants make "m" moves, each making one in the time interval $(t, t+1)$. Trail levels at the end of a cycle (at time $t+n$) are a function of the trail levels at the beginning of the cycle, the tour constructed by the elitist ant, and the tours made by the top ranked ants, and they are calculated as:

$$\tau_{ij}(t+n) = (1-\varphi)\,\tau_{ij}(t) + \lambda\Delta\tau_{ij}^{+} + \Delta\tau_{ij}^{r} \quad (12)$$

in the mentioned equation, the variable of φ is the coefficient of decay ($0 \le \varphi \le 1$) [52], denoting the persistence of the trail. $\Delta\tau_{ij}^{+}$ is the incremental trail level corresponding to the solution found by the elite ant of ψ^{+}. ρ shows an adjustable parameter in the range $0 \le \rho \le 1$. That the change in the trail level of the path *i-j* ($\Delta\tau_{ij}^{\mu}$), when opted with the ant ranked μ ($1 \le \mu \le \lambda$), is calculated with:

$$\Delta\tau_{ij}^{\mu} = \frac{R}{f(\psi^{\mu})} \quad (13)$$

wherein $f(\psi^{\mu})$ is the fitness value of the solution created by the ant ranked μ, and R is a magnitude regulating the contribution of the top ranked ants named the pheromone reward factor [53]. The path *i-j* may be selected by more than one ant. Therefore, the total increase in the trail level of the path ($\Delta\tau_{ij}^{r}$) is given by:

$$\Delta\tau_{ij}^{r} = \sum_{\lambda=1}^{\lambda-1} \Delta\tau_{ij}^{\mu} \quad (14)$$

2.5. Hybrid radial basis function neural network models

The radial basis neural network for the present is known as a model including the input, hidden, and output layers. Thus, convergence in the model of RBF will be high [54]. The neurons embedded in the input layer operate the parameters to the hidden layer, where the Gaussian function indicates the hidden layer's neurons. The RBF neural network must reflect on the input signals near the center point in the relevant function. The outcomes of the resulting hidden layer are headed to a layer of output, in which it is mainly a linear function that easily enacts [55].

As shown in Fig. 3, the network inputs are located in the input layer. Also, w denotes weight which w_0 is the weight of the output layer. The function of Gaussian (φ) used in this study appears to be Eq. (15):

$$\varphi_i = exp\left(-\frac{\|t-c_i\|}{\sigma_i^2}\right) \quad (15)$$

$$Y = W^T\varphi = \sum_{i=1}^{q} w_i\varphi(\|t-c_i\|) \quad (16)$$

Wherein, φ_i represents output of i^{th} node of hidden layer; c_i shows Prototype center of i^{th} Gaussian function, σ denotes spread rate parameter; $\|t-c_i\|$ represents the distance between input t and c_i. The RBF neural network as a modifiable strategy for dedicating the spread rate and the neuron number of hidden layers is to be adjusted by determining parameters to increase the efficiency. Meanwhile, defining the appropriate composition of neuron numbers and spread rate would be calculated using two algorithms of research. Both hybrid RBF-GWO RBF-ACO frameworks are operated to devise the capable model. The GWO and ACO would compute the optimal number of neurons within the hidden layer and the spread rate in the RBF structure.

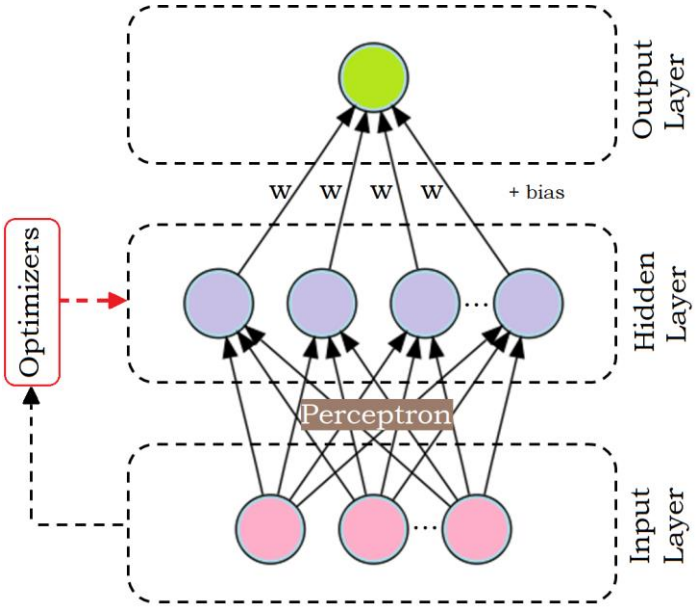

Fig. 3. Radial Basis Function structure coupling optimizers

2.6. Investigating the performance of modeling using the criteria

The criteria used to examine the performance of the hybrid RBF frameworks are described in Table 2. In Table 2, the p_N denotes forecasted magnitude; t_n is n^{th} pattern; $\bar{t}$ shows the objective amounts relevant to the N^{th}; $\bar{p}$ is the target values averaged as estimated. Further, the n_{train} and n_{test}, respectively, show the data number in the training and testing stages.

Table 2. The indices for evaluation of developed RBF models

Evaluator name	Symbol	Equation	Description
Mean absolute error	MAE	$\frac{1}{N}\sum_{n=1}^{N}\lvert p_n - t_n\rvert$	Low is desirable
Variance account factor	OBJ	$\left(\frac{n_{train}-n_{test}}{n_{train}+n_{test}}\right)\frac{RMSE_{train}+MAE_{test}}{R^2_{train}+1} + \left(\frac{2n_{train}}{n_{train}+n_{test}}\right)\frac{RMSE_{test}-MAE_{test}}{R^2_{test}+1}$	Low is desirable
Root mean squared error	RMSE	$\sqrt{\frac{1}{N}\sum_{n=1}^{N}(p_n - t_n)^2}$	Low is desirable
Variance account factor	VAF	$\left(1-\frac{var(t_n-y_n)}{var(t_n)}\right)*100$	High is desirable
Pearson's correlation coefficient	R	$\left(\frac{\sum_{n=1}^{N}(t_n-\bar{t})(p_n-\bar{p})}{\sqrt{[\sum_{n=1}^{N}(t_n-\bar{p})^2][\sum_{n=1}^{N}(p_n-\bar{p})^2]}}\right)^2$	High is desirable

3. Result and discussion

The developed RBF neural networks called RBF-GWO and RBF-ACO for finding pile settlement rates predicted have been generated and exhibited in this sector. The number of neurons found optimally for the hidden layer in both frameworks was obtained 70 (with one hidden layer). In this situation, the complexity and cost factors of neural network modeling should be effective for simulating

accurately what was done through the MATLAB environment. Figure 4 provides a scatter plot indicating the distribution of measured pile settlement rates in the KVMRT project with 70 percent and 30 percent for training and testing phases, respectively.

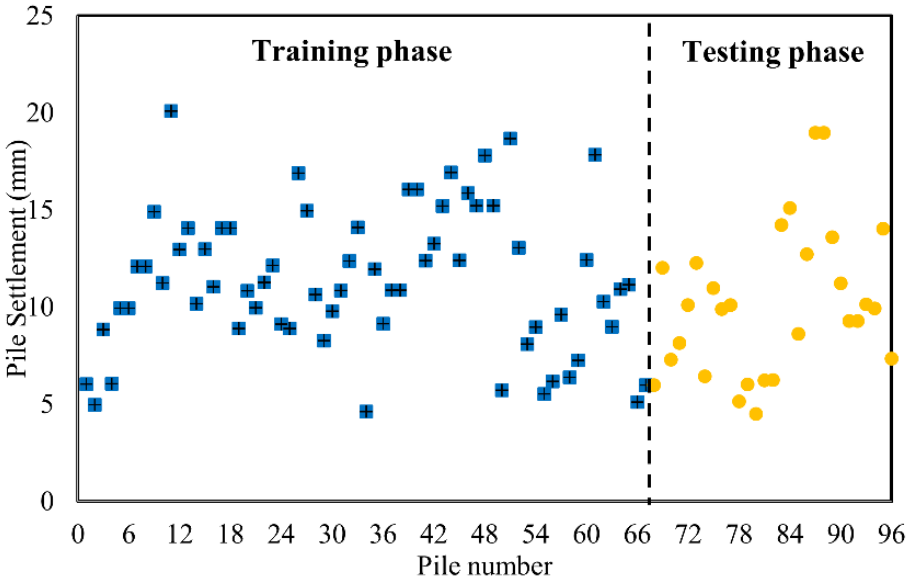

Fig. 4. Measured pile settlement data in the KVMRT project

Fig. 5 indicates the estimated and observed relationship of piles movements via the R and RMSE index correlation value.

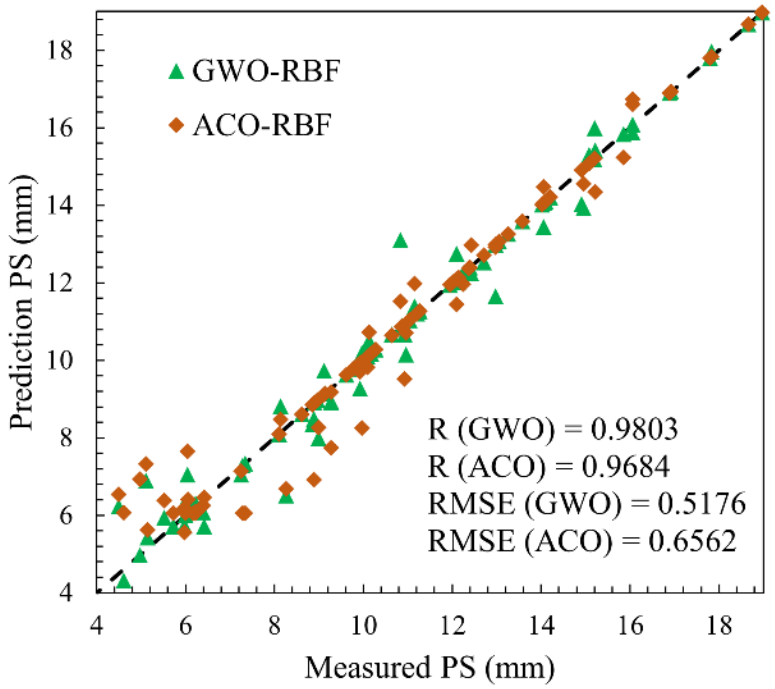

Fig. 5. The scatter plot of measurement and predictive modeling

As shown in Fig. 5, the RFB-GWO has proved the appropriate rate for both R and RMSE marks 1.23 and 26.78 percent higher than RFB-ACO, respectively. To optimize the number of neurons embedded in the hidden layer, GWO could have done better since the scattered points around the best-fit line are closer than those

associated with ACO. Notably, the piles related to high numbers were modeled close to real measurements with minimum errors well. This fact can be explained by applying 70 percent of data to train neural networks.

In this regard, Table 3 has depicted the capability of modeling for each hybrid model using the *VAF, R, MAE, OBJ,* and *RMSE* indices (described in Table 2). The outcomes of both phases as the training and testing show a similar pattern. In the training phase, the optimization algorithm of GWO has acted better by comparing all indices with the values desirable with the results of ACO. The MAE index has taken the most discrepancy, with about 30 percent in favor of GWO. While the difference in the outputs of *VAF* and *R*-correlation indexes has not attracted attention with a slight difference. Identically, all indicators of R, OBJ, MAE, VAF, and RMSE related to the testing phase for RBF- GWO have been placed at a desirable level compared to RBF-ACO by the maximum difference in *RMSE* as 37.4 percent. Meanwhile, the index of OBJ containing the error indexes of R, RMSE, MAE in both phases of train and test that can be seen as the comprehensive criterion to give a better perspective of the modeling process, showed that RBF- GWO serves better modeling with about 0.37 mm mistake in modeling pile settlement.

Table 3. Obtained values of performance evaluators for PS modeling

Models			**RBF-ACO**	**RBF-GWO**	**Difference (%)**
Spread rate			21.5651	68.4898	
Number of hidden layers neurons			70	70	
Assessment criteria	Training phase	*R*	0.9652	0.9772	1.24%
		RMSE	0.6757	0.5467	23.60%
		MAE	0.3474	0.2679	29.68%
		VAF	96.34	97.70	1.41%
	Testing phase	*R*	0.9735	0.986	1.28%
		RMSE	0.6089	0.4432	37.39%
		MAE	0.3182	0.2362	34.72%
		VAF	97.31	98.52	1.24%
OBJ			0.4189	0.3698	13.30%

Fig. 6 tries to indicate each pile's modeling mistakes rather than target values that are measured to have a good view of the accuracy of simulation models. As shown in Fig. 6, there are some positions where measurements and modeling lines are not coincidental. Moreover, most of the modeling is conducted correctly, as seen in two parts of testing and training. This diagram has depicted where and to what extent gaps exist between modeling and real measurements.

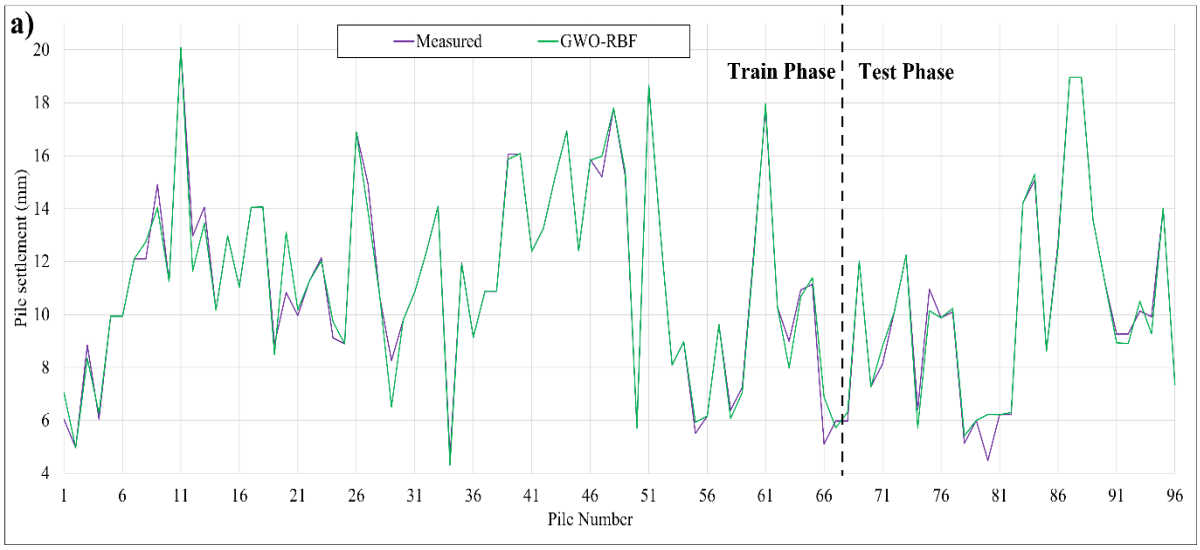

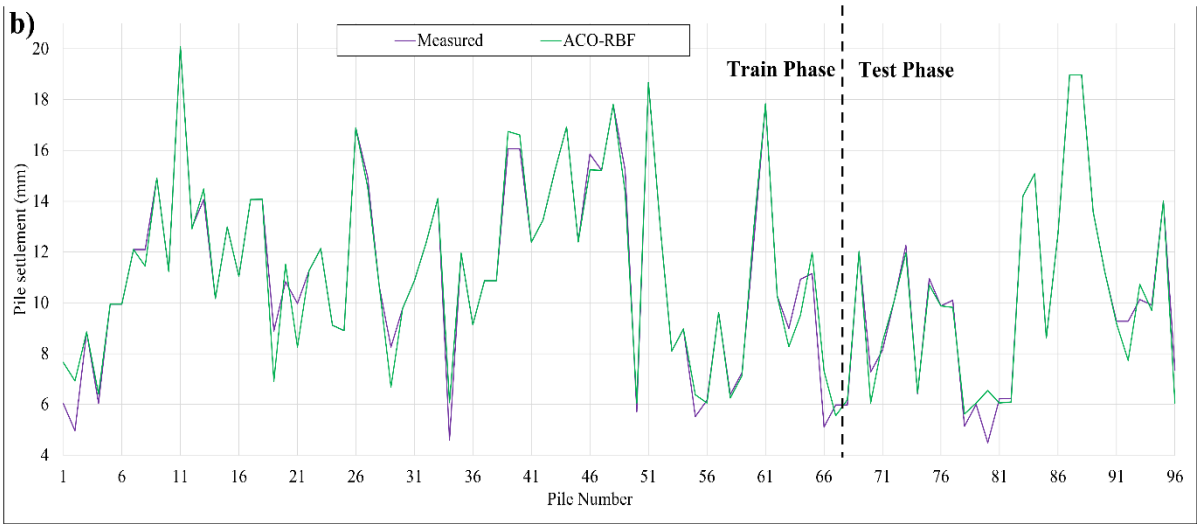

Fig. 6. Showing the difference of pile settlement measured and estimated by (a) RBF-GWO and (b) RBF-ACO

Fig. 7 presents a better view to analyze the performance of modeling. The mentioned diagram implies errors to reach the target for piles modeled according to the measured ones in terms of positive (overestimation) and negative (underestimation). Therefore, based on Figure 7, diagram (a) for RBF-GWO has shown mistakes in simulating pile movement that reaches the maximum of 35 percent in the training phase. However, the error rate has risen to 40 percent in the testing phase. On the other side, RBF-ACO (diagram b) can do defined duty to model pile settlement with mistakes higher than RBF-GWO. For the training phase, the error of RBF-ACO has closely bitten 45 percent. That this threshold has passed in the testing stage. But in mentioned stage the prediction error line of RBF-ACO is flatter than RBF-GWO.

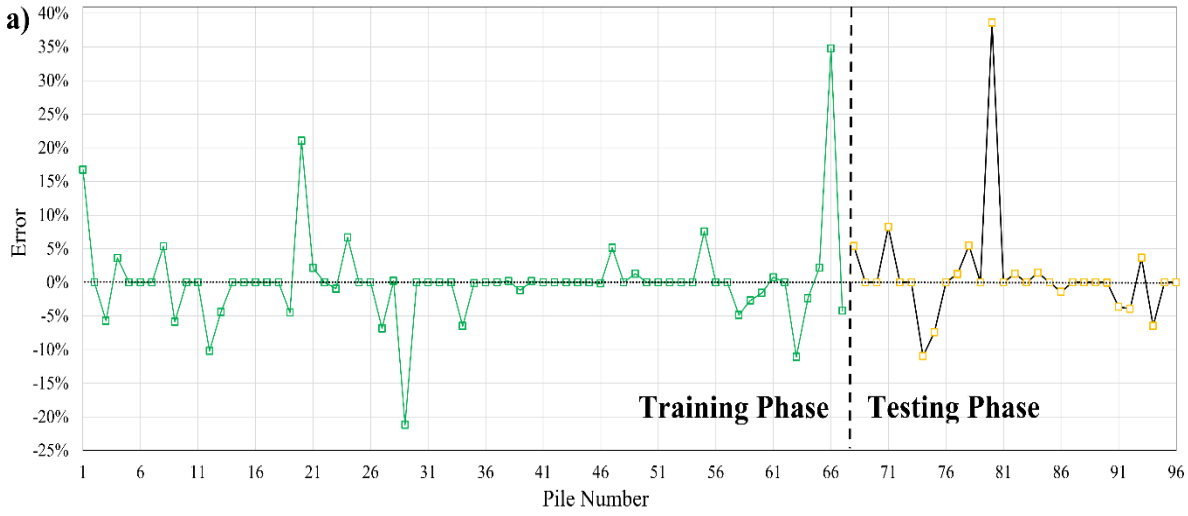

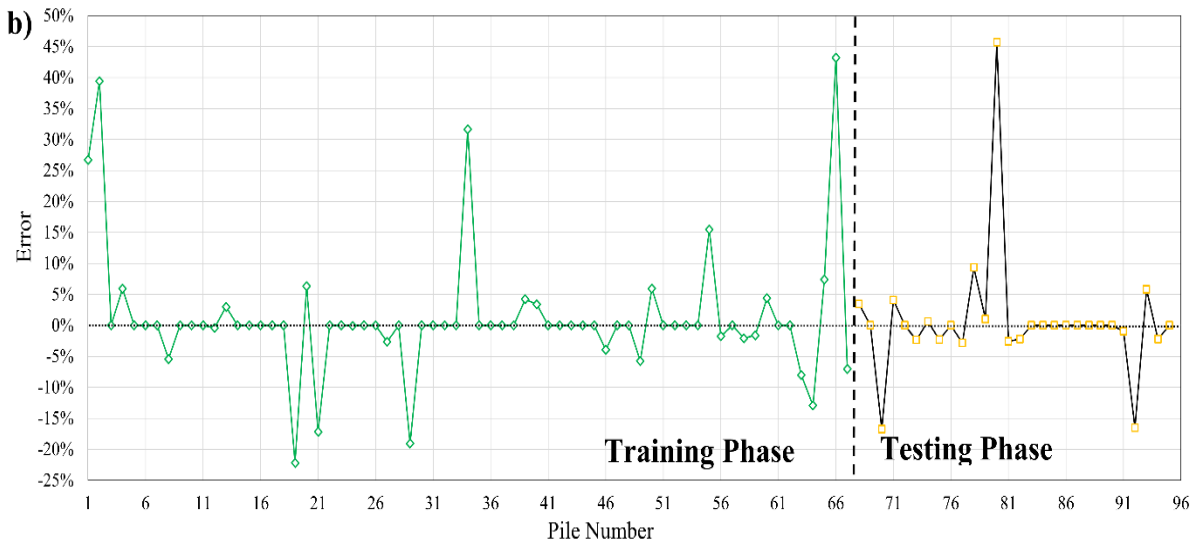

Fig. 7. The error of PS modeling in (a) RBF-GWO and (b) RBF-ACO

Fig. 8 indicates the normal distribution of errors for both RBF-GWO and RBF-ACO hybrid models. Also, the frequency of error classes is brought up in this figure.

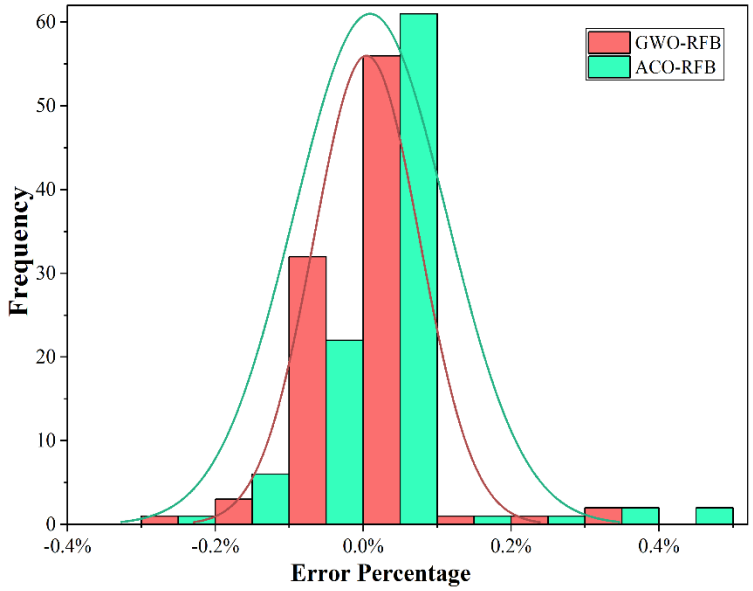

Fig. 8. Normal distribution of errors in modeling for both hybrid models

Interestingly, despite the fact that neural network with GWO has had the better performance in simulating the pile settlement with suitable results, the RBF-ACO has better error distribution with a bell-shaped normal distribution diagram. On the other hand, the RBF-GWO framework has a wide area of errors that this matter has led to the reduction of error histograms' height rather than RBF-ACO.

4. Conclusion

Piles' Foundations have been critical projects requiring columns to carry loads and masses to the ground base. Especially, the heavy structures such as bridges and

tall buildings entail being surveyed in terms of any dangers that could be a recipe for disaster. Existing pile settlement as a defective feature of projects has to be analyzed to facilitate construction over the long. For this reason, appraising the pile settlement rate mathematically can reduce the risk of failure in mega projects. Therefore, the present paper aims to model the pile settlement using the Radial Basis Function (RBF) neural network. In this way, Grey Wolf Optimization (GWO) and Ant Colony Optimization (ACO) were used to find the optimal number of neurons in the hidden layer to reduce the complexity and cost of network calculations. To utilize hybrid models of RBF-GOW and RBF-ACO, pile tests and ground properties were obtained for Klang Valley Mass Rapid Transit (KVMRT) 's transportation project in Malaysia.

Both proposed frameworks had outstanding capability to appraise the dependent variable of Pile Settlement (PS), where the R value for the training phase was obtained on averagely 0.9860 and 0.9735 in the test level for RBF-GOW and RBF-ACO, respectively, signifies the difference of 1.28 percent. To check the spreading of samples data adjacent to the best-fit line, the lower pile numbers of both frameworks showed the same performance, according to Fig. 7.

To sum up, RBF-GWO could get an acceptable score by the indices for evaluating each strategy. Statistically, the RBF-GWO framework, with the desirable values of R, RMSE, MAE, and VAF at 0.9803, 0.5176, 0.2583, 97.992, outperformed than RBF-ACO with those of 0.9684, 0.6562, 0.3386, and 96.733, respectively, that the highest difference is related to the *MAE* with 31 percent. For the training stage that includes 70 percent of data, RBF-GWO could hit the 0.9772 R-value just 1.24 percent higher than RBF-ACO's performance. Finally, the holistic index of the *OBJ* evaluator, consisting of the main error and correlation criteria of *R, RMSE, MAE* indexes, proves that RBF-ACO and RBF-GWO have been obtained, respectively, 0.4189 and 0.3698, with a 13.30 percent difference. To sum up, employing the hybrid models with desirable outcomes with the aid of smart software-based approaches can reduce the costs of physical experiments and simultaneously increase the accuracy of predicting mechanical features of crucial concrete material.

REFERENCES

[1] L. Mu, M. Huang, and R. J. Finno, "Tunnelling effects on lateral behavior of pile rafts in layered soil," *Tunnelling and Underground Space Technology*, vol. 28, pp. 192–201, 2012.

[2] H. G. Poulos and L. T. Chen, "Pile response due to excavation-induced lateral soil movement," *Journal of Geotechnical and geoenvironmental engineering*, vol. 123, no. 2, pp. 94–99, 1997.

[3] N. Loganathan, H. G. Poulos, and K. J. Xu, "Ground and pile-group responses due to tunnelling," *Soils and Foundations*, vol. 41, no. 1, pp. 57–67, 2001.

[4] Z. Zhang, M. Huang, C. Xu, Y. Jiang, and W. Wang, "Simplified solution for tunnel-soil-pile interaction in Pasternak's foundation model," *Tunnelling and Underground Space Technology*, vol. 78, pp. 146–158, 2018.

[5] T. Gerheim Souza Dias and A. Bezuijen, "Data analysis of pile tunnel interaction," *JOURNAL OF GEOTECHNICAL AND GEOENVIRONMENTAL ENGINEERING*, vol. 141, no. 12, 2015.

[6] R. J. Mair and M. G. Williamson, "The influence of tunnelling and deep excavation on piled foundations," *Geotechnical Aspects of Underground Construction in Soft Ground*, pp. 21–30, 2014.

[7] J. Cherian, "Determining the amount of earthquake displacement using differential synthetic aperture radar interferometry (D-InSAR) and satellite images of Sentinel-1 A: A case study of Sarpol-e Zahab city," *Advances in Engineering and Intelligence Systems*, vol. 1, no. 01, 2022.

[8] Z. Nurlan, "A novel hybrid radial basis function method for predicting the fresh and hardened properties of self-compacting concrete," *Advances in Engineering and Intelligence Systems*, vol. 1, no. 01, 2022.

[9] H. Cheng, S. Kitchen, and G. Daniels, "Novel hybrid radial based neural network model on predicting the compressive strength of long-term HPC concrete," *Advances in Engineering and Intelligence Systems*, vol. 1, no. 02, 2022.

[10] Q. Zhang and M. Afzal, "Prediction of the elastic modulus of recycled aggregate concrete applying hybrid artificial intelligence and machine learning algorithms," *Structural Concrete*, 2021.

[11] R. S. Benemaran and M. Esmaeili-Falak, "Optimization of cost and mechanical properties of concrete with admixtures using MARS and PSO," *Computers and Concrete*, vol. 26, no. 4, pp. 309–316, 2020.

[12] G. Russo and C. Viggiani, "Factors controlling soil-structure interaction for piled rafts," *Darmstadt Geotechnics, Darmstadt Univ. of Technology*, vol. 4, pp. 297–322, 1998.

[13] B. El-Garhy, A. A. Galil, A.-F. Youssef, and M. A. Raia, "Behavior of raft on settlement reducing piles: Experimental model study," *Journal of Rock Mechanics and Geotechnical Engineering*, vol. 5, no. 5, pp. 389–399, 2013.

[14] A. M. Alnuaim, H. El Naggar, and M. H. El Naggar, "Performance of micropiled raft in sand subjected to vertical concentrated load: centrifuge modeling," *Canadian Geotechnical Journal*, vol. 52, no. 1, pp. 33–45, Jan. 2015, doi: 10.1139/cgj-2014-0001.

[15] D. Park and J. Lee, “Interaction effects on load-carrying behavior of piled rafts embedded in clay from centrifuge tests,” *Canadian Geotechnical Journal*, vol. 52, no. 10, pp. 1550–1561, Oct. 2015, doi: 10.1139/cgj-2014-0336.

[16] J. B. Burland, R. J. R. Hancock, and J. Burland, *Underground car park at the House of Commons, London: geotechnical aspects*. Building Research Establishment, 1977.

[17] H. G. Poulos and E. H. Davis, *Pile foundation analysis and design*, no. Monograph. 1980.

[18] E. C. Leong and M. F. Randolph, “Finite element modelling of rock-socketed piles,” *International journal for numerical and analytical methods in geomechanics*, vol. 18, no. 1, pp. 25–47, 1994.

[19] R. A. Douglas and R. Butterfield, “Pile group elastic load response prediction: friction piles embedded in cohesive soils,” *Canadian Geotechnical Journal*, vol. 21, no. 3, pp. 587–592, 1984.

[20] Y. Zhang, X. Hu, D. D. Tannant, G. Zhang, and F. Tan, “Field monitoring and deformation characteristics of a landslide with piles in the Three Gorges Reservoir area,” *Landslides*, vol. 15, no. 3, pp. 581–592, 2018.

[21] Y. Zhang, D. C. Richardson, O. S. Barnouin, P. Michel, S. R. Schwartz, and R.-L. Ballouz, “Rotational failure of rubble-pile bodies: influences of shear and cohesive strengths,” *The Astrophysical Journal*, vol. 857, no. 1, p. 15, 2018.

[22] W. F. Che, T. M. H. Lok, S. C. Tam, and H. Novais-Ferreira, “Axial capacity prediction for driven piles at Macao using artificial neural network.” AA Balkema Publishers, Leiden, 2003.

[23] H. Liu, T. J. Li, and Y. F. Zhang, “The application of artificial neural networks in estimating the pile bearing capacity,” 1997.

[24] M. Shanbeh, D. Najafzadeh, and S. A. H. Ravandi, “Predicting pull-out force of loop pile of woven terry fabrics using artificial neural network algorithm,” *Industria Textila*, vol. 63, no. 1, pp. 37–41, 2012.

[25] I.-M. Lee and J.-H. Lee, “Prediction of pile bearing capacity using artificial neural networks,” *Computers and geotechnics*, vol. 18, no. 3, pp. 189–200, 1996.

[26] A. M. Hanna, G. Morcous, and M. Helmy, “Efficiency of pile groups installed in cohesionless soil using artificial neural networks,” *Canadian Geotechnical Journal*, vol. 41, no. 6, pp. 1241–1249, 2004.

[27] R. Sarkhani Benemaran, M. Esmaeili-Falak, and H. Katebi, “Physical and numerical modelling of pile-stabilised saturated layered slopes,” *Proceedings of the Institution of Civil Engineers-Geotechnical Engineering*, pp. 1–16, 2020.

[28] L. Huang, W. Jiang, Y. Wang, Y. Zhu, and M. Afzal, “Prediction of long-term compressive strength of concrete with admixtures using hybrid swarm-based algorithms,” *Smart Structures and Systems*, vol. 29, no. 3, pp. 433–444, 2022.

[29] A. T. C. Goh, “Pile Driving Records Reanalyzed Using Neural Networks,” *Journal of Geotechnical Engineering*, vol. 122, no. 6, pp. 492–495, Jun. 1996, doi: 10.1061/(ASCE)0733-9410(1996)122:6(492).

[30] C. I. Teh, K. S. Wong, A. T. C. Goh, and S. Jaritngam, “Prediction of pile capacity using neural networks,” *Journal of computing in civil engineering*, vol. 11, no. 2, pp. 129–138, 1997.

[31] M. Shariati *et al.*, “A novel hybrid extreme learning machine–grey wolf optimizer (ELM-GWO) model to predict compressive strength of concrete with partial replacements for cement,” *Engineering with Computers*, 2020, doi: 10.1007/s00366-020-01081-0.

[32] H. Gao and Z. Jun-Wei, “Estimation of pile settlement applying hybrid radial basis function network with BBO, ALO, and GWO optimization algorithms,” *Journal of Applied Science and Engineering*, vol. 25, no. 6, pp. 1031–1044, 2022.

[33] S. Rajasekaran and J. S. Chitra, “Ant colony optimisation of spatial steel structures under static and earthquake loading,” *Civil Engineering and Environmental Systems*, vol. 26, no. 4, pp. 339–354, 2009.

[34] S. M. Kalami Heris and H. Khaloozadeh, “Ant Colony Estimator: An intelligent particle filter based on,” *Engineering Applications of Artificial Intelligence*, vol. 28, pp. 78–85, Feb. 2014, doi: 10.1016/j.engappai.2013.11.005.

[35] H. Bendu, B. Deepak, and S. Murugan, “Application of GRNN for the prediction of performance and exhaust emissions in HCCI engine using ethanol,” *Energy conversion and management*, vol. 122, pp. 165–173, 2016.

[36] V. K. Alilou and F. Yaghmaee, “Application of GRNN neural network in non-texture image inpainting and restoration,” *Pattern Recognition Letters*, vol. 62, pp. 24–31, 2015.

[37] A. Zendehboudi and A. Tatar, “Utilization of the RBF network to model the nucleate pool boiling heat transfer properties of refrigerant-oil mixtures with nanoparticles,” *Journal of Molecular Liquids*, vol. 247, pp. 304–312, 2017.

[38] R. Sarkhani Benemaran, M. Esmaeili-Falak, and A. Javadi, “Predicting resilient modulus of flexible pavement foundation using extreme gradient boosting based optimized models,” *International Journal of Pavement Engineering*, 2022, doi: 10.1080/10298436.2022.2095385.

[39] M. A. Shahin, H. R. Maier, and M. B. Jaksa, “Predicting settlement of shallow foundations using neural networks,” *Journal of Geotechnical and Geoenvironmental Engineering*, vol. 128, no. 9, pp. 785–793, 2002.

[40] J. Wu, J. Long, and M. Liu, “Evolving RBF neural networks for rainfall prediction using hybrid particle swarm optimization and genetic algorithm,” *Neurocomputing*, vol. 148, pp. 136–142, 2015.

[41] L. Xu, F. Qian, Y. Li, Q. Li, Y. Yang, and J. Xu, "Resource allocation based on quantum particle swarm optimization and RBF neural network for overlay cognitive OFDM System," *Neurocomputing*, vol. 173, pp. 1250–1256, 2016.
[42] A. W. Hatheway, "The complete ISRM suggested methods for rock characterization, testing and monitoring; 1974–2006." Association of Environmental & Engineering Geologists, 2009.
[43] D. Simon, "Biogeography-based optimization," *IEEE transactions on evolutionary computation*, vol. 12, no. 6, pp. 702–713, 2008.
[44] S. Mirjalili, S. M. Mirjalili, and A. Lewis, "Grey wolf optimizer," *Advances in engineering software*, vol. 69, pp. 46–61, 2014.
[45] J.-L. Deneubourg, S. Aron, S. Goss, and J. M. Pasteels, "The self-organizing exploratory pattern of the argentine ant," *Journal of insect behavior*, vol. 3, no. 2, pp. 159–168, 1990.
[46] M. Dorigo, V. Maniezzo, and A. Colorni, "Ant system: optimization by a colony of cooperating agents," *IEEE Transactions on Systems, Man, and Cybernetics, Part B (Cybernetics)*, vol. 26, no. 1, pp. 29–41, 1996.
[47] F. A. C. Viana, G. I. Kotinda, D. A. Rade, and V. Steffen Jr, "Tuning dynamic vibration absorbers by using ant colony optimization," *Computers & Structures*, vol. 86, no. 13–14, pp. 1539–1549, 2008.
[48] C. V Camp and B. J. Bichon, "Design of space trusses using ant colony optimization," *Journal of structural engineering*, vol. 130, no. 5, pp. 741–751, 2004.
[49] İ. Aydoğdu and M. P. Saka, "Ant colony optimization of irregular steel frames including elemental warping effect," *Advances in Engineering Software*, vol. 44, no. 1, pp. 150–169, 2012.
[50] V. Maniezzo, L. M. Gambardella, and F. De Luigi, "Ant colony optimization," in *New Optimization Techniques in Engineering*, Springer, 2004, pp. 101–121.
[51] M. Dorigo, M. Birattari, and T. Stutzle, "Ant colony optimization," *IEEE computational intelligence magazine*, vol. 1, no. 4, pp. 28–39, 2006.
[52] A. Uğur and D. Aydin, "An interactive simulation and analysis software for solving TSP using Ant Colony Optimization algorithms," *Advances in Engineering software*, vol. 40, no. 5, pp. 341–349, 2009.
[53] R. Moeini and M. H. Afshar, "Layout and size optimization of sanitary sewer network using intelligent ants," *Advances in Engineering Software*, vol. 51, pp. 49–62, 2012.
[54] W. Sun, D. Liu, J. Wen, and Z. Wu, "Modeling of MEMS gyroscope random errors based on grey model and RBF neural network," *J. Navig. Position*, vol. 5, pp. 9–13, 2017.
[55] S. Seshagiri and H. K. Khalil, "Output feedback control of nonlinear systems using RBF neural networks," *IEEE Transactions on Neural Networks*, vol. 11, no. 1, pp. 69–79, 2000.